

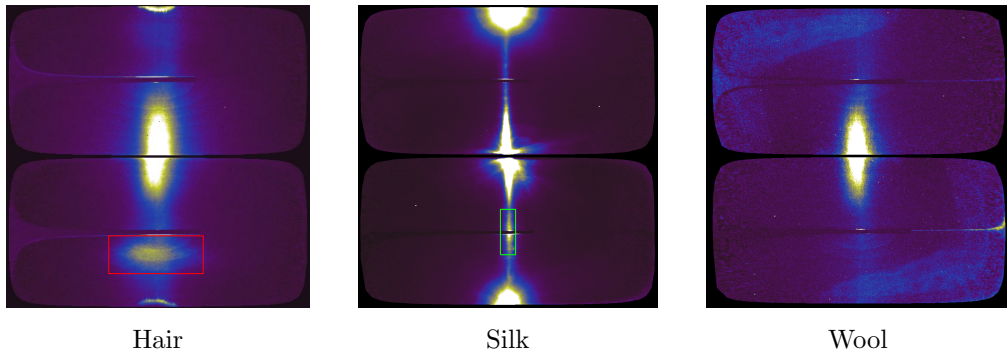
# Supplementary Materials for “Fiber-Based Appearance Models for Fabrics”

Section 1 presents casual observations that motivated us not to include the TRT mode in our fiber scattering model. Section 2 presents details of the normalized Gaussian function used to construction our fiber scattering model, especially the formula for the normalization factor. Section 3 discusses how we choose evaluation points we use to define the parameter rescaling functions in Section 5 of the paper. Section 4 discusses how the photographs of the fabric samples were processed. Lastly, Section 5 compares photographs and renderings of the six cloth samples in 492 scene configurations that were not used for fitting parameters in Section 7 of the paper.

## 1 Evidence for Dropping the TRT Mode in Cloth Fibers

In Section 4 of the paper, we construct a light scattering model using a framework for BCSDF of hair fibers. An important decision we made is not to include the TRT or higher modes in our model. In this section, we present casual observations that convinced us of its validity.

We used a device that can capture the sphere of outgoing scattered light from fibers whose specifics are detailed in [1]. Here, we provide pictures taken from the receiving bowl of the device, warped into the  $(\theta_o, \phi_o)$ -plane, showing the scattered light from a Caucasian hair (used in [1]), a silk fiber of the Silk sample in the fiber, and a wool fiber from a fabric (not used in the paper).



Here, we emphasize the TRT mode, present in scattered light from the hair, with a red rectangle. We can see that such a structure is not visible in the scattered light from the silk fiber and the wool fiber. We might say that the blob surrounded by the green rectangle is the TRT mode of the silk, but observe that it is very small when compared to the TRT blot of the hair. (The two big blobs on the top and the bottom edges of the silk fiber’s image are light spilt directly on the device from the light source. They are not part of the scattered light.)

## 2 Normalized Gaussian in $\theta$

In Section 4 of the paper, we define a fiber scattering function for textile fibers. The definition makes uses of a normalized Gaussian function in  $\theta$  defined as follows:

$$\bar{g}(\theta; \mu, \sigma) = \frac{g(\theta; \mu, \sigma)}{G(\mu, \sigma)}$$

where  $g(\theta; \mu, \sigma)$  denotes the Gaussian distribution with mean  $\mu$  and standard deviation  $\sigma$ , and  $G(\mu, \sigma)$  is a normalization factor chosen to satisfy the energy conservation constraint

$$\int_{-\pi/2}^{\pi/2} \bar{g}(\theta; \mu, \sigma) \cos^2 \theta \, d\theta \leq 1.$$

We define  $G(\mu, \sigma)$  by approximating  $\cos^2 \theta$  from above by the polynomial

$$Q(\theta) = 0.002439\theta^8 - 0.04301\theta^6 + 0.3322\theta^4 - 0.999745\theta^2 + 1.0001 \geq \cos^2 \theta,$$

and setting

$$G(\mu, \sigma) = \int_{-\pi/2}^{\pi/2} g(\theta; \mu, \sigma) Q(\theta) \, d\theta.$$

The values of  $G$  can be computed by analytically integrating the product of a Gaussian function with a polynomial using the following lemma.

**Lemma 2.1.** *Let  $P(x) = p_0 + p_1x + \cdots + p_kx^k$ . The indefinite integral of  $P(x)g(x; \mu, \sigma)$  is given by*

$$\frac{A}{2} \operatorname{erf}\left(\frac{x - \mu}{\sqrt{2}\sigma}\right) - \sigma^2 B(x)g(x; \mu, \sigma) + C \quad (1)$$

where  $B(x) = b_0 + b_1x + \cdots + b_{k-1}x^{k-1}$ ,

$$b_j = \begin{cases} p_k, & j = k - 1, \\ p_{k-1} + \mu b_{k-1}, & j = k - 2, \\ p_{j+1} + \mu b_{j+1} + (j+2)\sigma^2 b_{j+2}, & 0 \leq j < k - 2, \end{cases}$$

and  $A = p_0 + \mu b_0 + \sigma^2 b_1$ .

*Proof.* Expression (1) has three terms. The derivative of the constant  $C$  is 0. The derivative of the first term is:

$$\frac{A}{2} \left\{ \operatorname{erf}\left(\frac{x - \mu}{\sqrt{2}\sigma}\right) \right\}' = \frac{A}{2} \cdot \frac{2}{\sqrt{\pi}} \cdot e^{\frac{-(x-\mu)^2}{2\sigma^2}} \cdot \frac{1}{\sqrt{2}\sigma} = Ag(x; \mu, \sigma). \quad (2)$$

The derivative of the second term of Expression (1) is:

$$-\sigma^2 B'(x)g(x; \mu, \sigma) - \sigma^2 B_k(x)g'(x; \mu, \sigma). \quad (3)$$

The first term of Expression (3) is:

$$-\sigma^2 B'_k(x, \mu, \sigma)g(x; \mu, \sigma) = \left( \sum_{j=1}^{k-1} -j\sigma^2 b_j x^{j-1} \right) g(x; \mu, \sigma). \quad (4)$$

The second term of Expression (3) is:

$$\begin{aligned} -\sigma^2 B_k(x, \mu, \sigma) g'(x, \mu, \sigma) &= -\sigma^2 B_k(x, \mu, \sigma) \frac{-2(x - \mu)}{2\sigma^2} g(x; \mu, \sigma) \\ &= (x - \mu) \left( \sum_{j=0}^{k-1} b_j x^j \right) g(x; \mu, \sigma). \end{aligned} \quad (5)$$

As a result, we see that the derivative of Expression (1) is a polynomial multiplied by  $g(x; \mu, \sigma)$ . We shall show that this polynomial is equal to  $P(x)$ . So, adding Expressions (2), (4), and (5), we have that the polynomial multiplied to  $g(x; \mu, \sigma)$  is:

$$\begin{aligned} A + \left( \sum_{j=0}^{k-2} -(j+1)\sigma^2 b_{j+1} x^j \right) + (x - \mu) \left( \sum_{j=0}^{k-1} b_j x^j \right) \\ = A - \sigma^2 b_1 - \mu b_0 + \sum_{j=1}^{k-2} (b_{j-1} - \mu b_j - (j+1)\sigma^2 b_{j+1}) x^j \\ + (b_{k-2} - \mu b_{k-1}) x^{k-1} + b_{k-1} x^k \\ = p_0 + \sum_{j=1}^{k-2} p_j x^j + p_{k-1} x^{k-1} + p_k x^k = P(x). \end{aligned}$$

The last line follows from the recurrence relation in the Lemma's statement.  $\square$

### 3 Evaluation Points for Parameter Rescaling Curves

In Section 5.5 of the paper, we define a rescaling function  $r_p$  for each parameter  $p$  in the hope that, after applying each to the corresponding parameter, it becomes easier to find a good learning rate for the optimization. The definition of  $r_p$  requires an increasing sequence of values  $c_1, c_2, \dots, c_k$ , where  $[c_1, c_k]$  should cover the domain of parameter  $p$ . In this section, we discuss what this increasing sequence is for each parameter.

In general,  $c_i$  takes the form  $c_i = a + b \cdot m^{i-1}$  for some constants  $a$ ,  $b$ , and  $m$ . We fix  $k = 9$ . We use the aforementioned formula to compute the elements only from  $c_2$  to  $c_8$ . We set  $c_1$  and  $c_9$  to be the lower bound and the upper bound of the parameter's domain, respectively. The values of the constants are given in the table below:

Parameter	$a$	$b$	$m$	$c_1$	$c_9$	Notes
$C_R$	1.02296	-0.032255	1.5403	0.001	0.999	We use $1 - (a + b \cdot m^{i-1})$ instead.
$\beta_R$	$-7.0^\circ$ ,	$8.0^\circ$	1.1	$1^\circ$	$10.0^\circ$	—
$C_{TT}$	1.02296,	-1.02197	0.64922	0.001	0.999	—
$\beta_{TT}$	$-0.91^\circ$ ,	$1.9^\circ$	1.5	$1^\circ$	$45.0^\circ$	—
$\gamma_{TT}$	$-0.91^\circ$ ,	$1.9^\circ$	1.5	$1^\circ$	$45.0^\circ$	—

The values computed from the above process are given in the following table:

	$C_R$	$\beta_R$	$C_{TT}$	$\beta_{TT}$	$\gamma_{TT}$
$c_1$	0.001000	1.000000	0.001000	1.000000	1.000000
$c_2$	0.026722	1.800000	0.359470	1.940000	1.940000
$c_3$	0.053566	2.680000	0.592206	3.365000	3.365000
$c_4$	0.094913	3.648000	0.743304	5.502500	5.502500
$c_5$	0.158599	4.712800	0.841401	8.708750	8.708750
$c_6$	0.256696	5.884080	0.905087	13.518125	13.518125
$c_7$	0.407794	7.172488	0.946434	20.732187	20.732187
$c_8$	0.640530	8.589737	0.973278	31.553281	31.553281
$c_9$	0.999000	10.000000	0.999000	45.000000	45.000000

In the paper, however, we stated that the range of  $\beta_{TT}$  is from  $10^\circ$  to  $45^\circ$ . This means that, when performing optimization, we clamp the  $\beta_{TT}$  value to  $10^\circ$  if it gets lower than  $10^\circ$ . The scaling curve is independent of this clamping and was computed using the above sequence of numbers.

## 4 Processing of Cloth Photographs

Here, we briefly describe the processing we performed on our photographs so that they could be compared directly to renderings of our cloth models. We began by exporting linearized images from the camera raw data for each photograph. After normalizing for differences in exposure and ISO between photographs, we derived a color matrix to account for characteristics of the camera sensor and the light source as follows. We photographed a Macbeth chart placed on our measurement apparatus and rendered a corresponding model of the chart under the same geometric configuration with accurate spectral reflectance. We then fit a matrix to apply to our photographs to minimize the sum of squared differences between the chart colors in the photo (after applying the matrix) and the render, constrained to exactly match the color of the white square of the rendered chart. The resulting color match is shown in Figure 1.

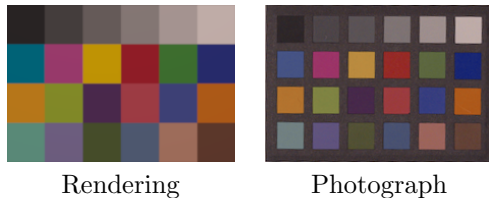


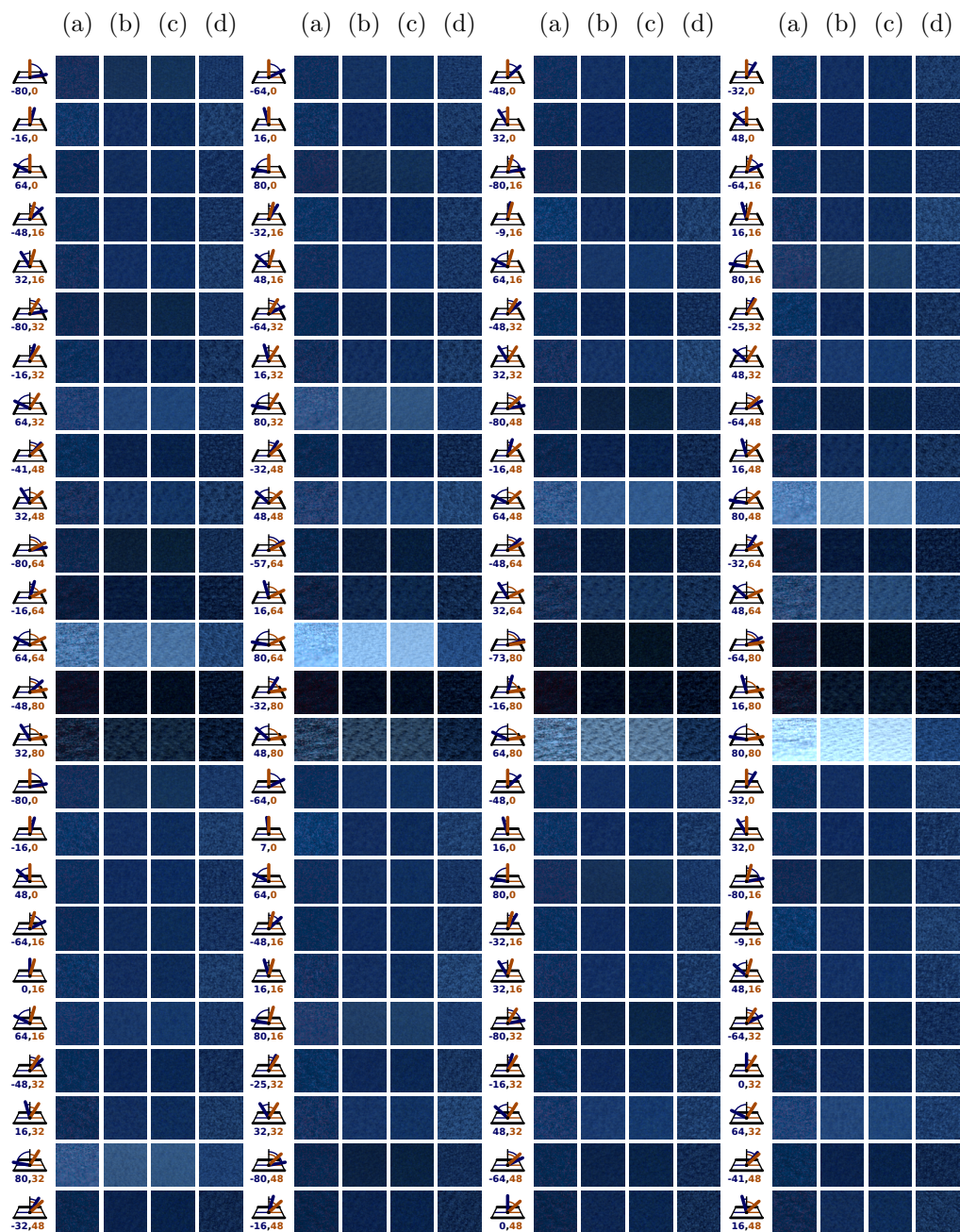
Figure 1: Rendered Macbeth chart and photograph after applying color matrix.

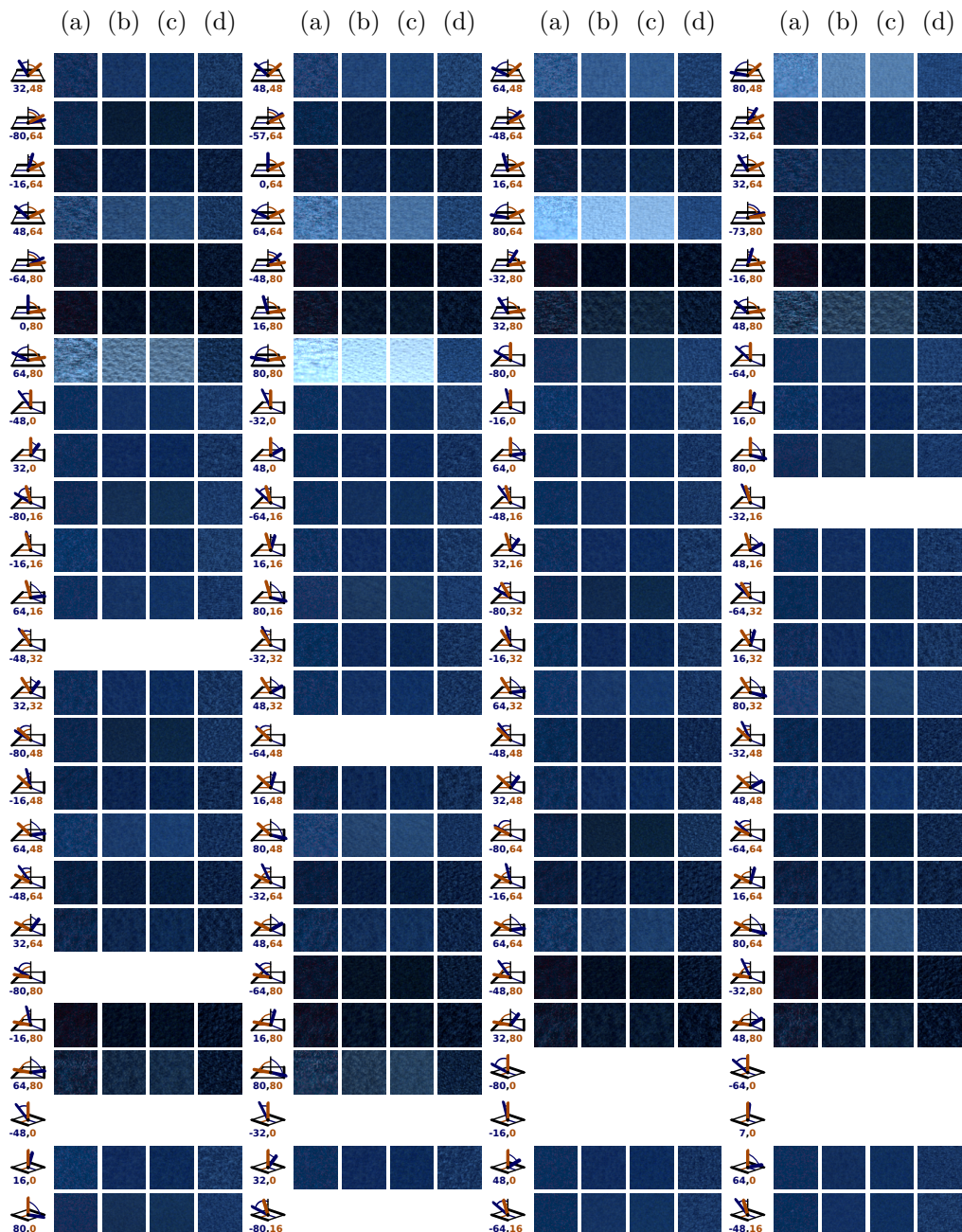
## 5 Full Evaluation of Planar Configurations

In the paper, we compare our photographs of six materials to fitted results for three rendering methods on the 16 viewing configurations used to fit the model parameters. For completeness, we present below all 492 scene configurations that were not used for fitting. Each configuration features (a) the photograph of the cloth sample, (b) the rendering of the Fiber/BCSDF model, (c) the rendering of the Volume/BCSDF model, and (d) the rendering of the Volume/microflake model. Configurations where the material was partially or completely occluded by the measurement apparatus in the photograph are omitted.

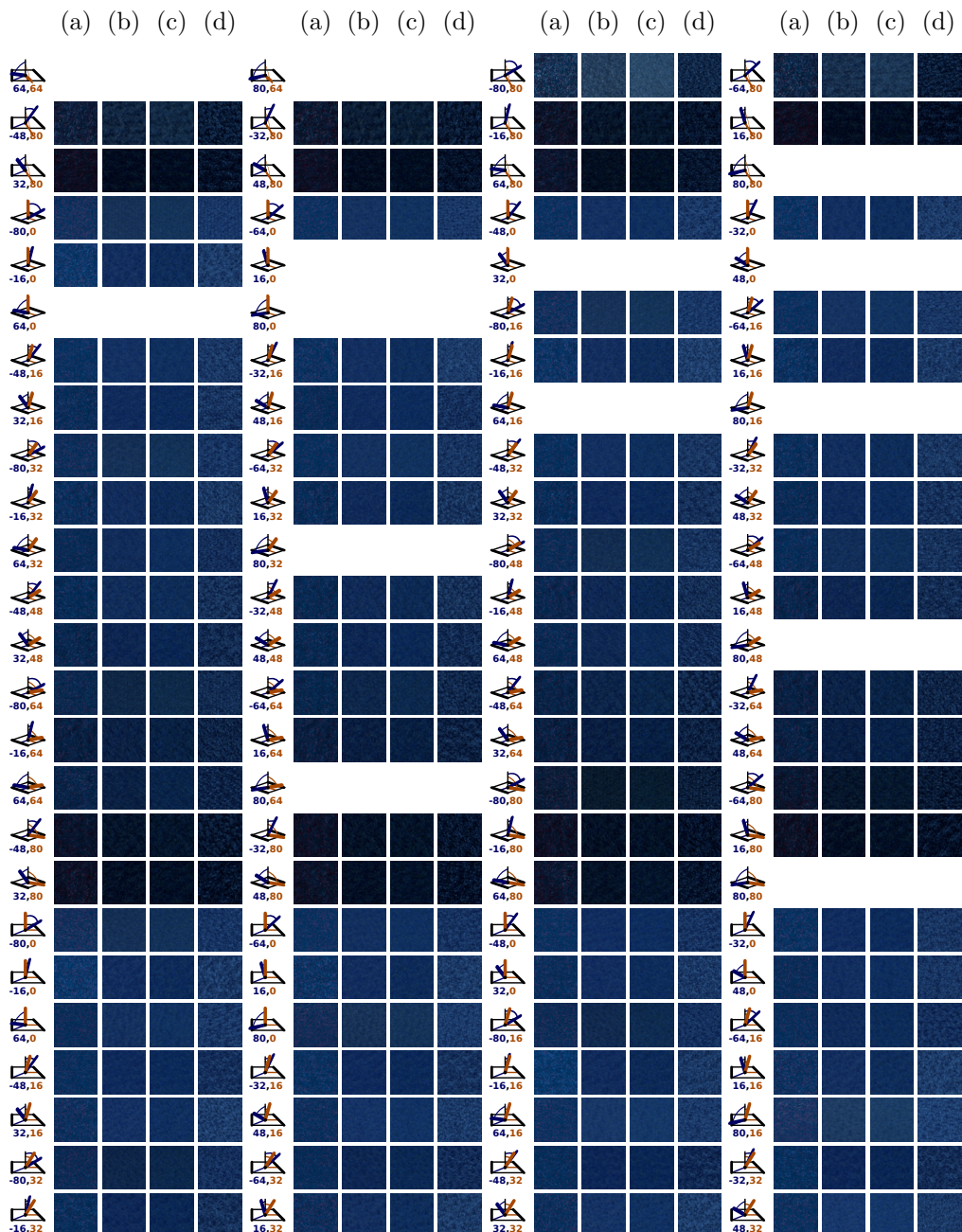
Due to time limitations, some of the models below were rendered with fewer samples than the corresponding images in the paper.

## 5.1 Fleece



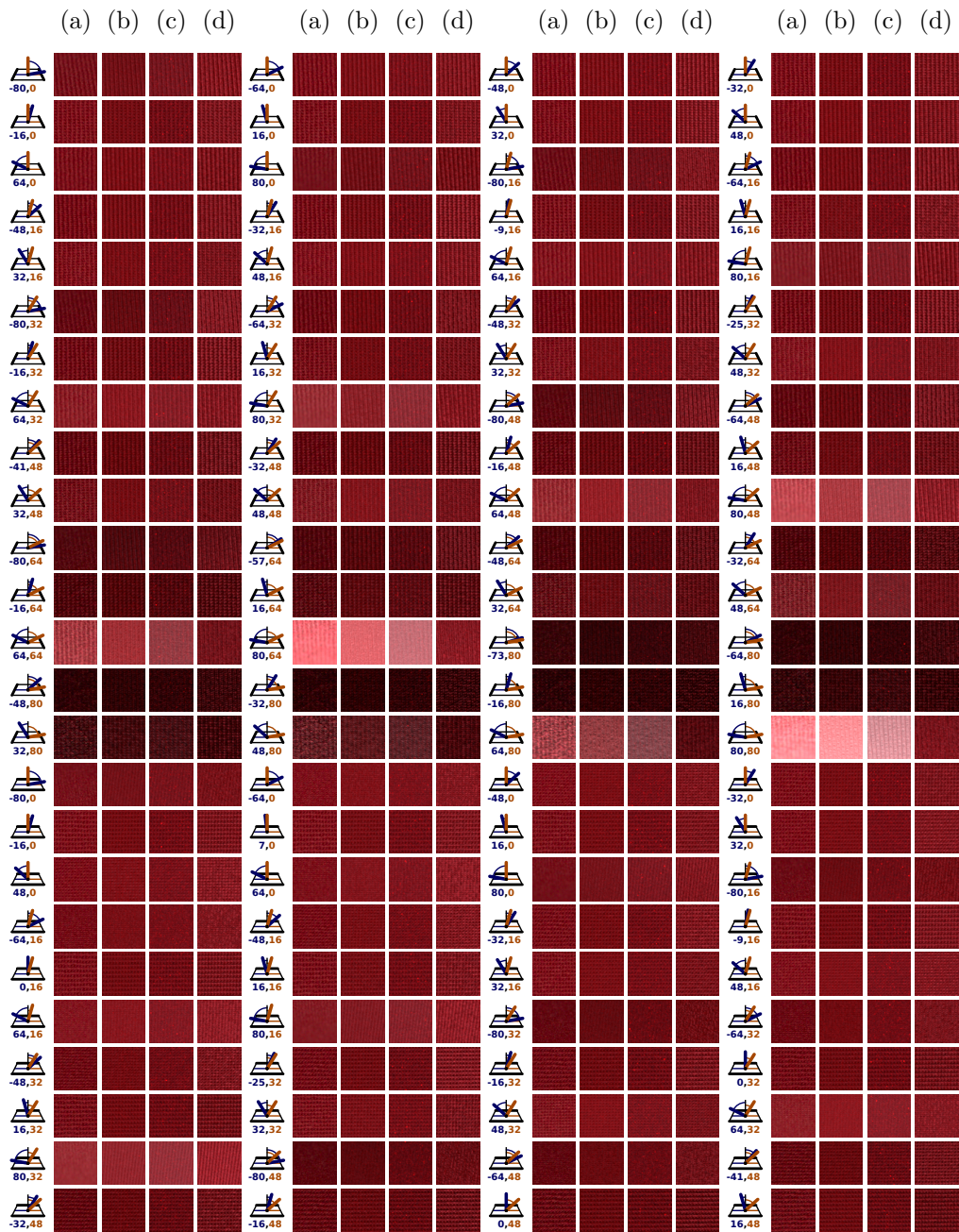


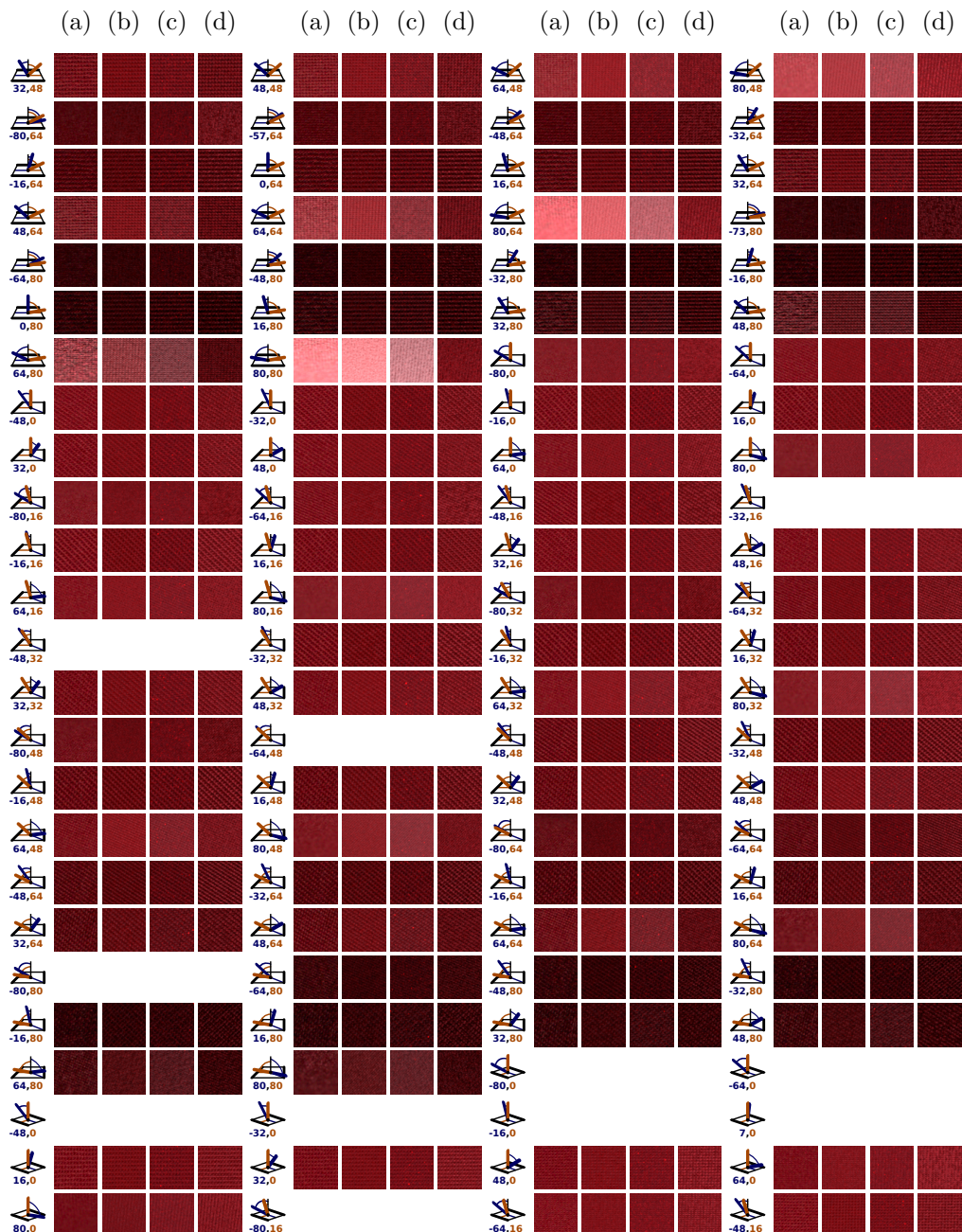


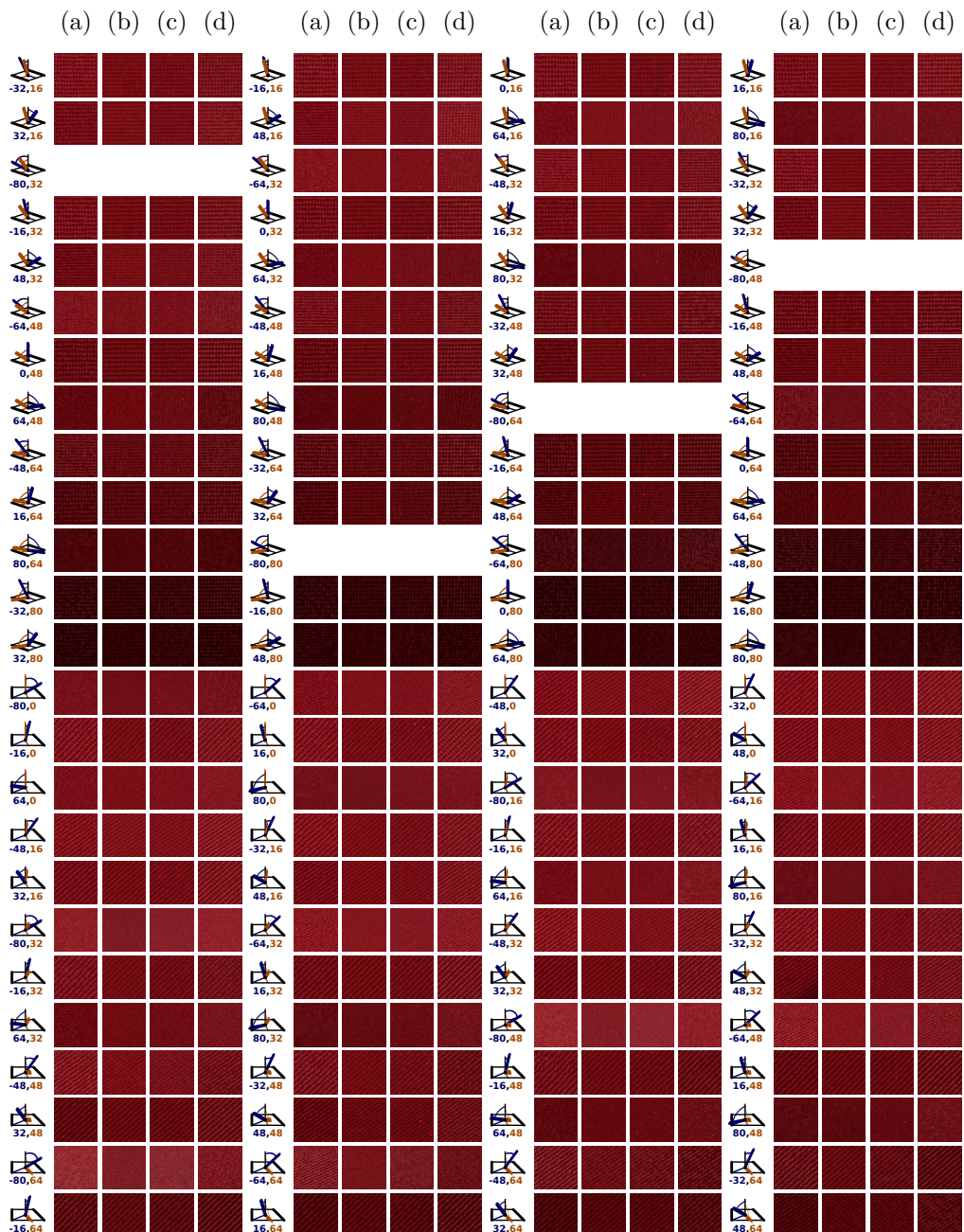


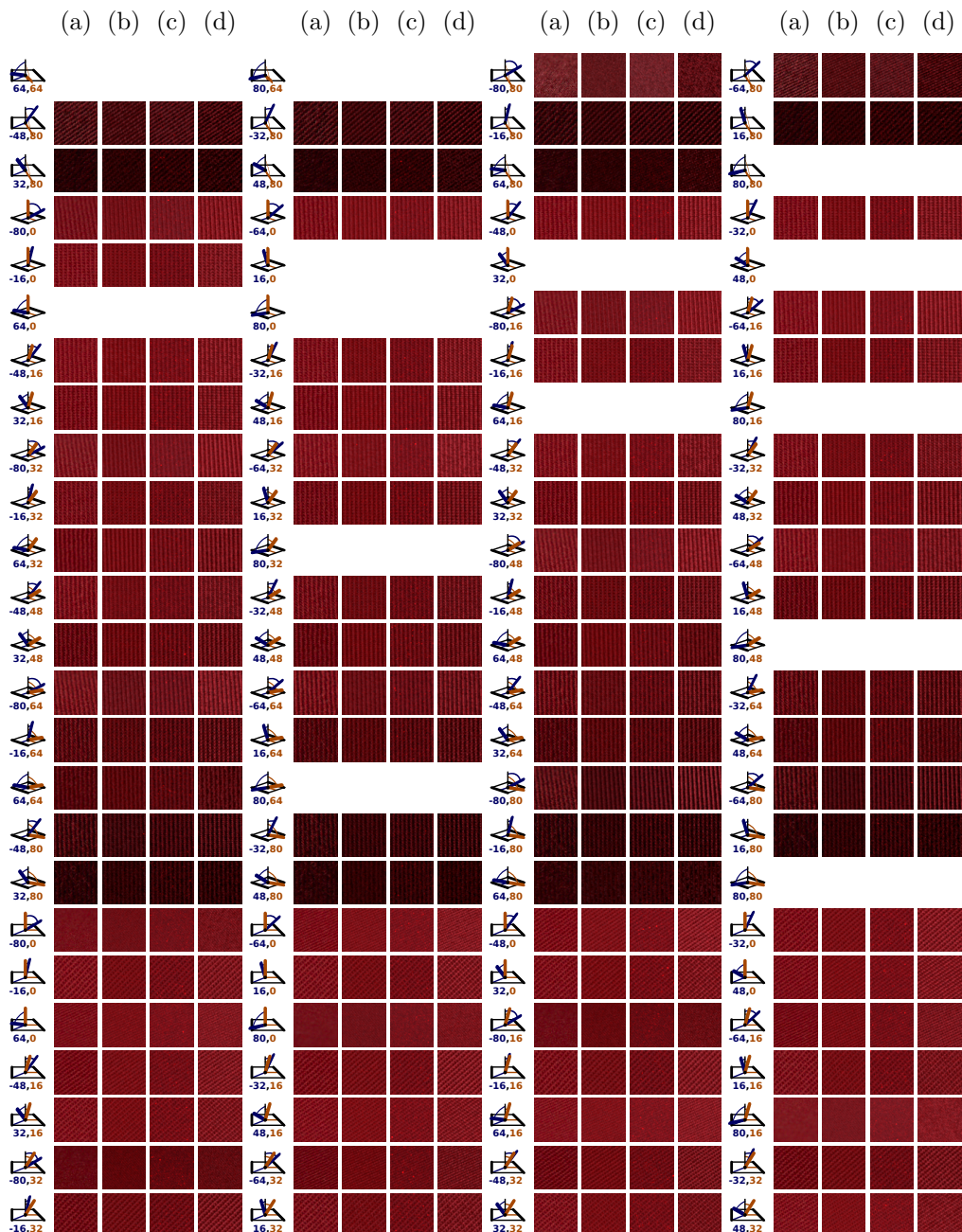


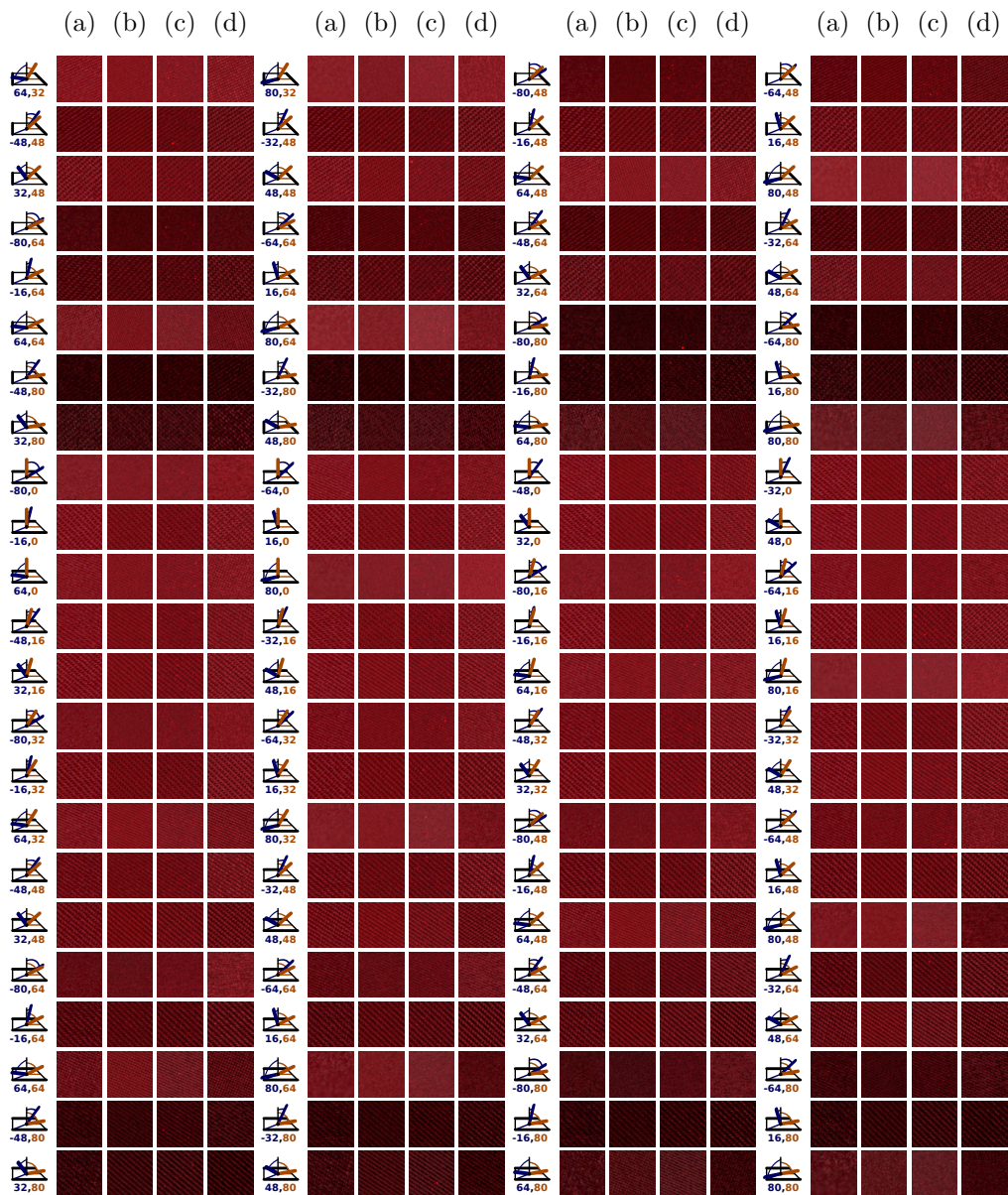
## 5.2 Gabardine



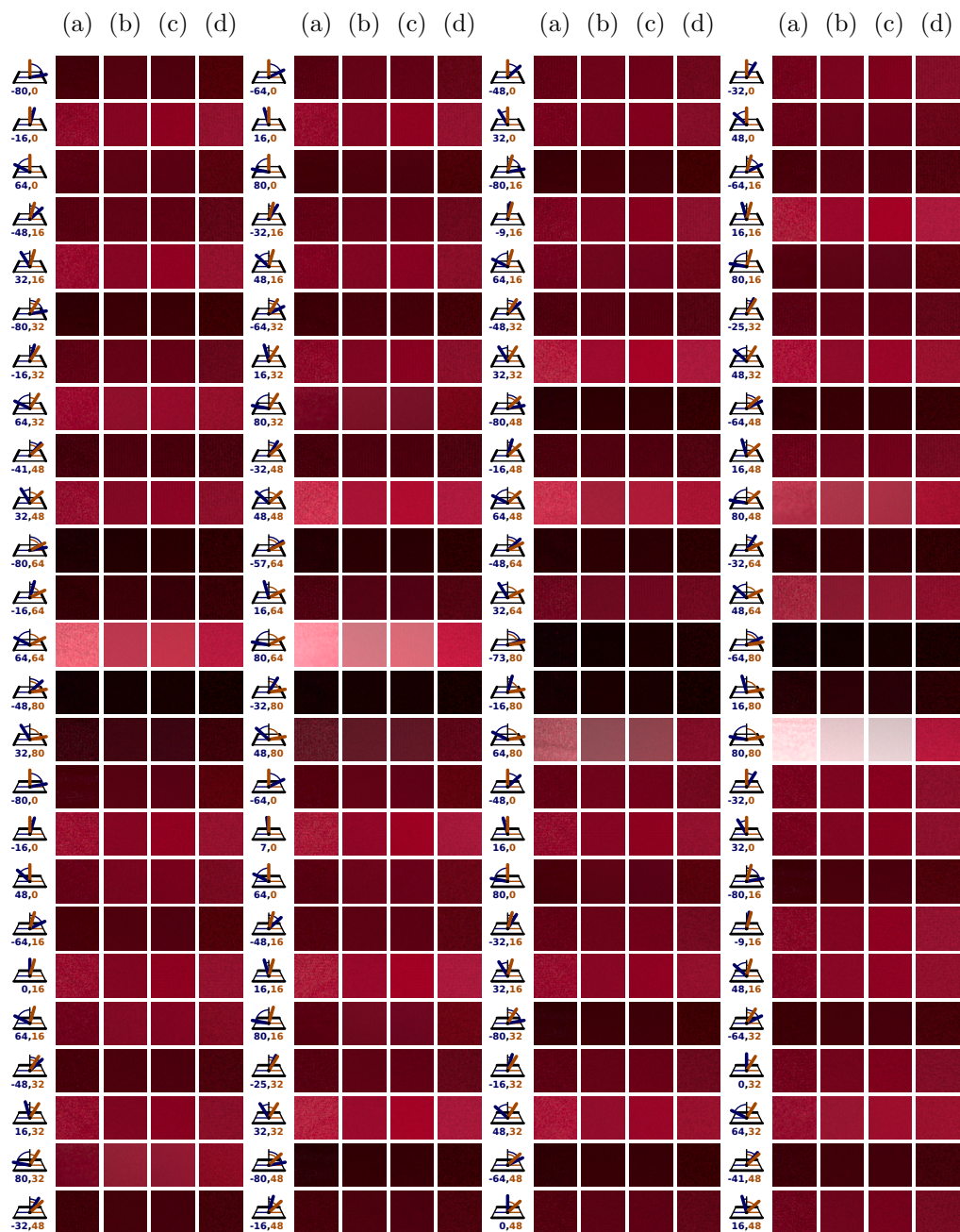


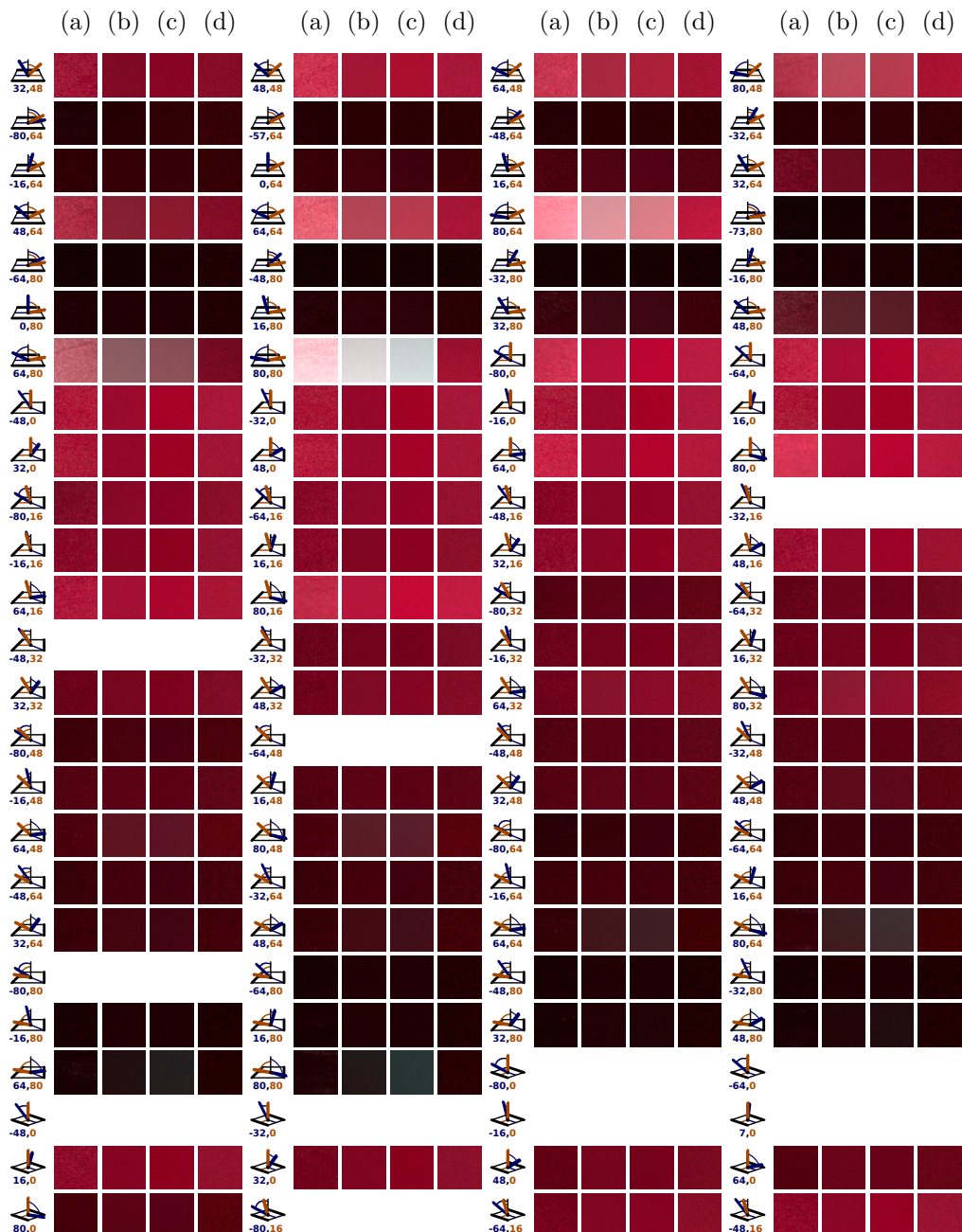


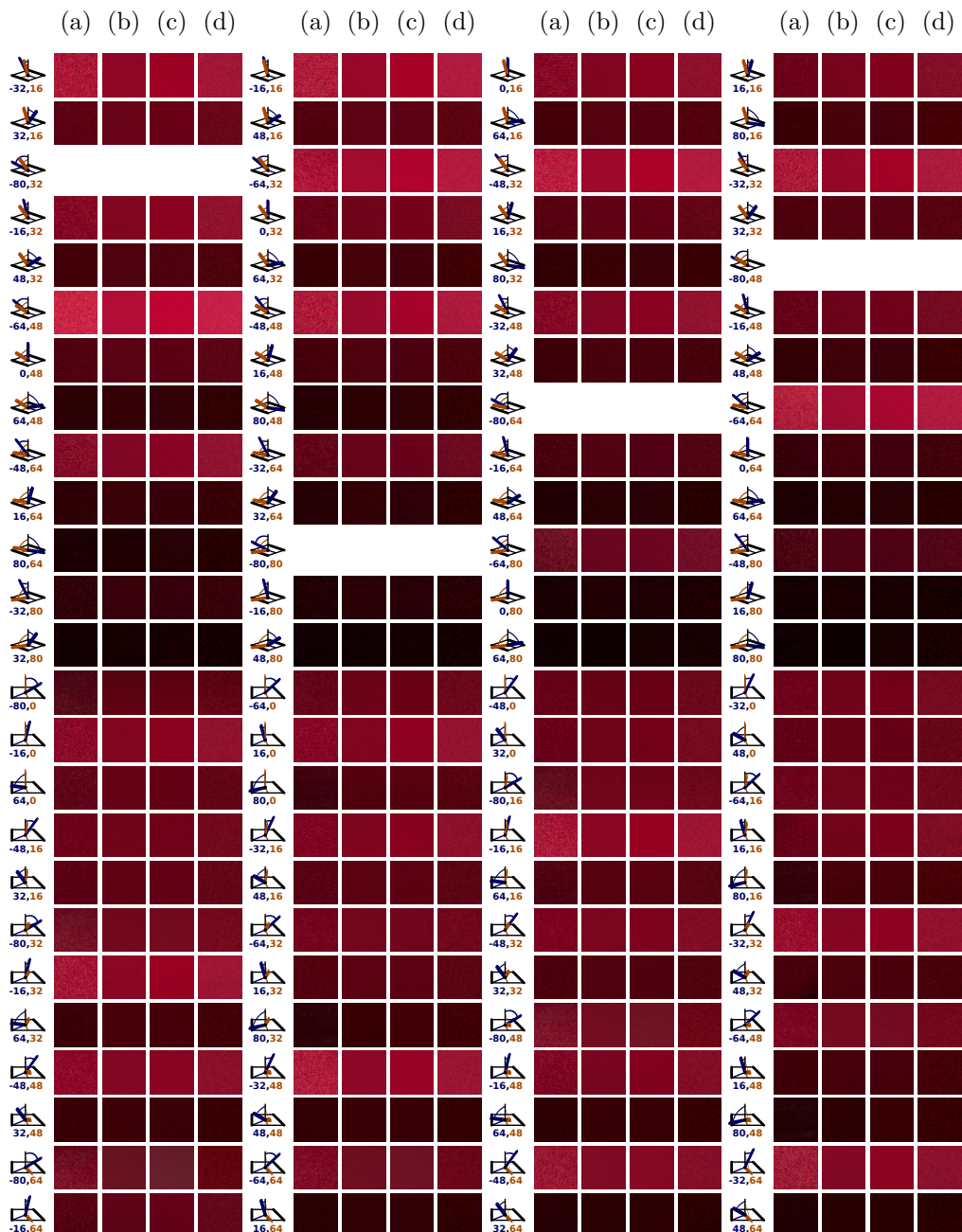


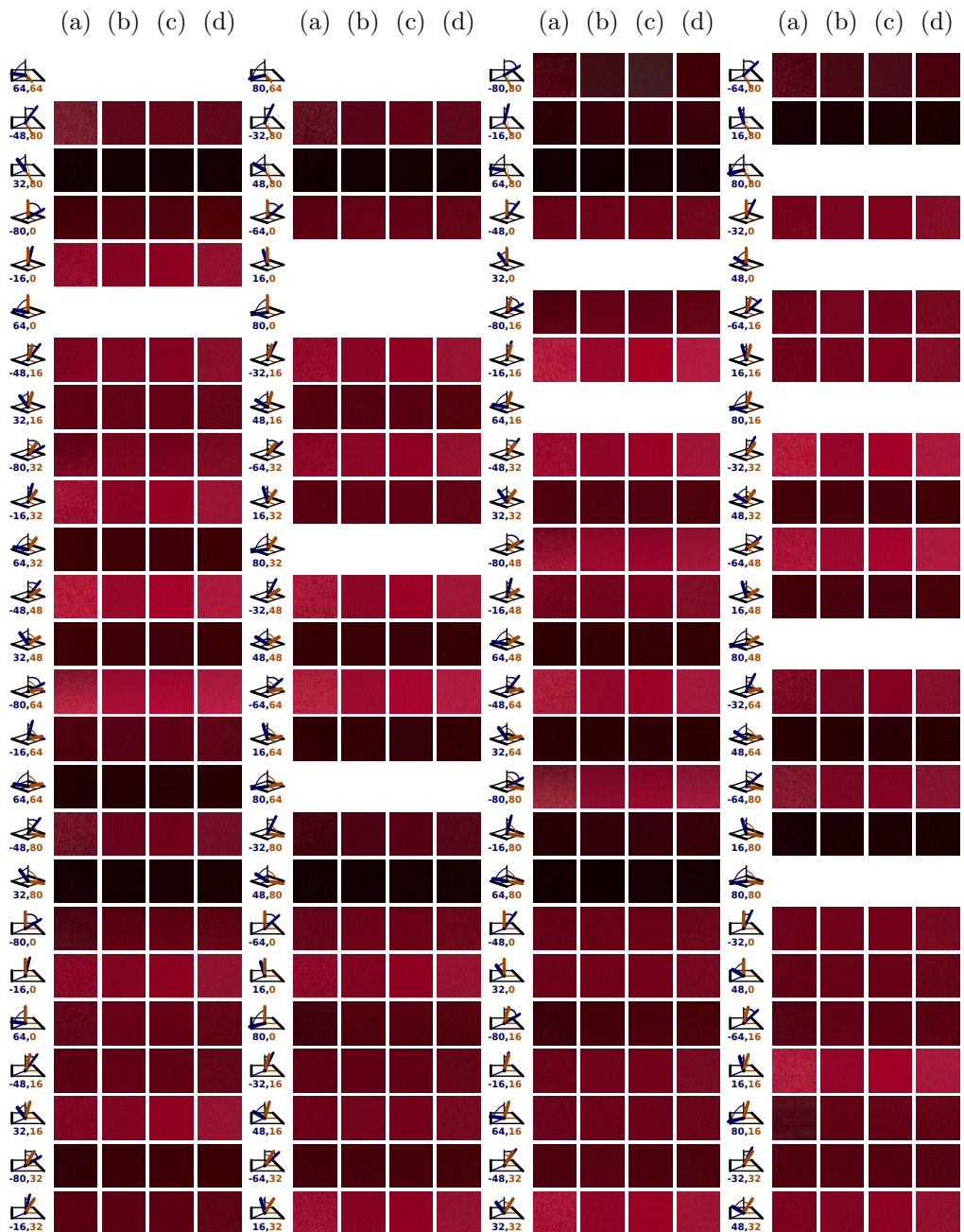


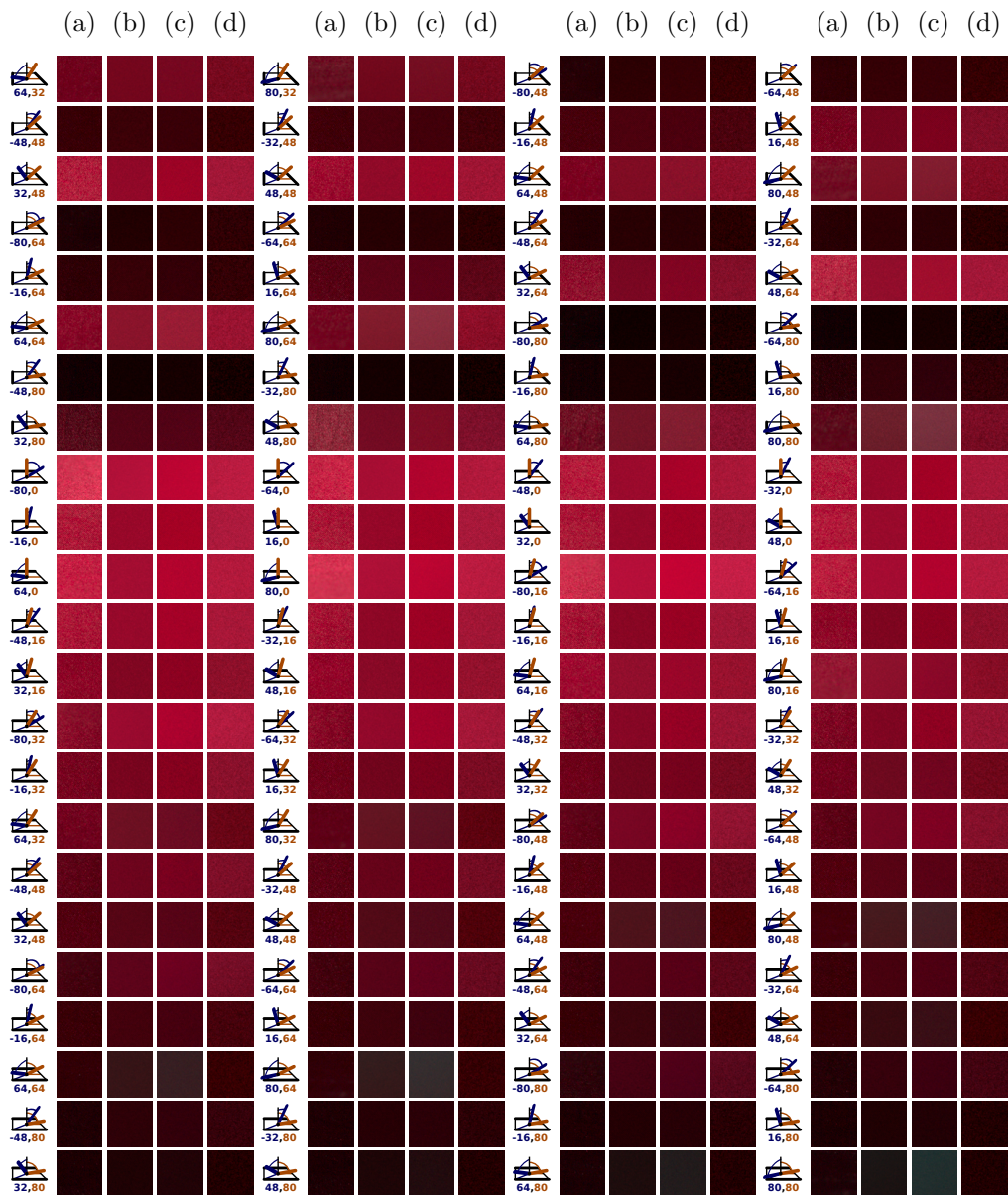
### 5.3 Silk



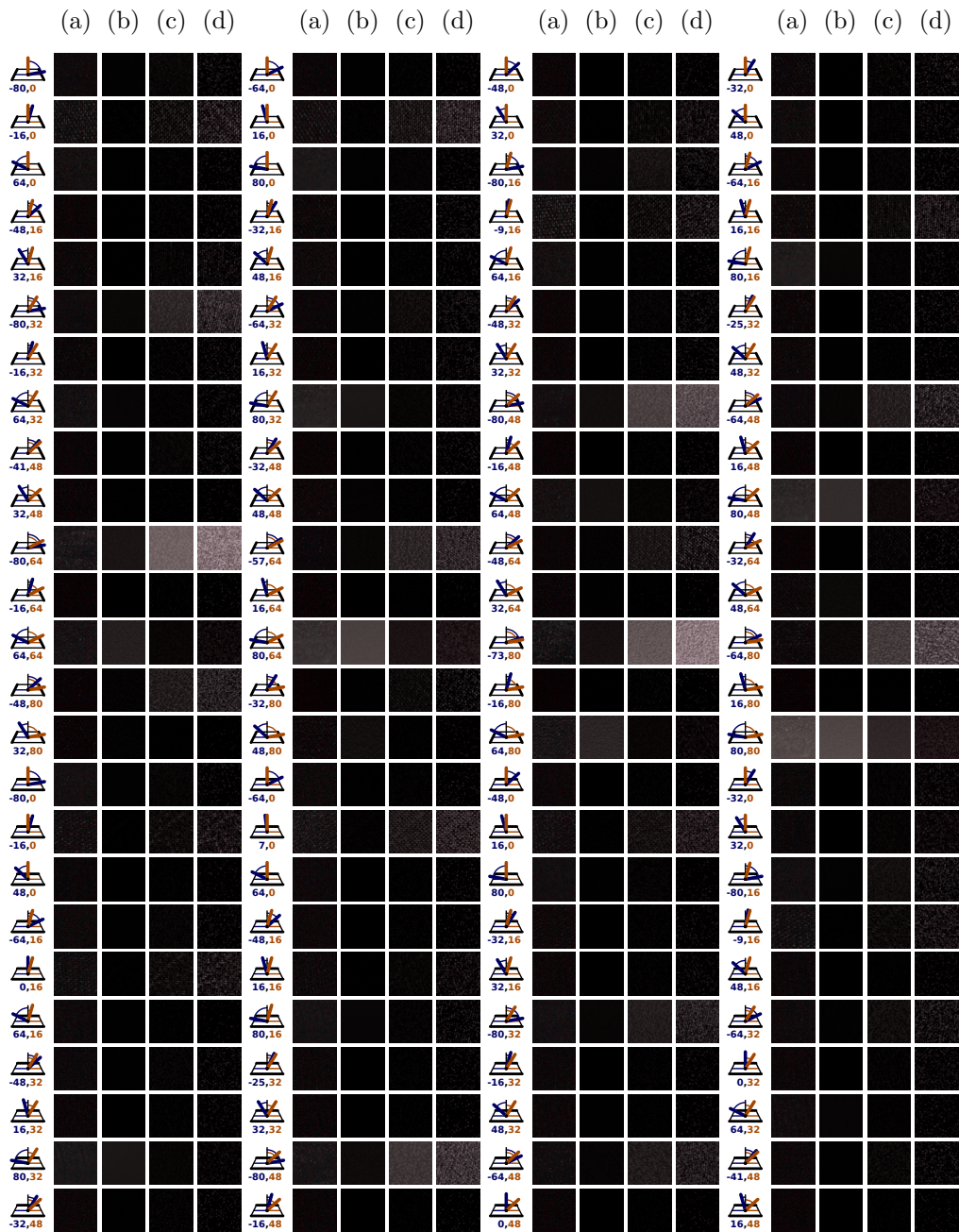


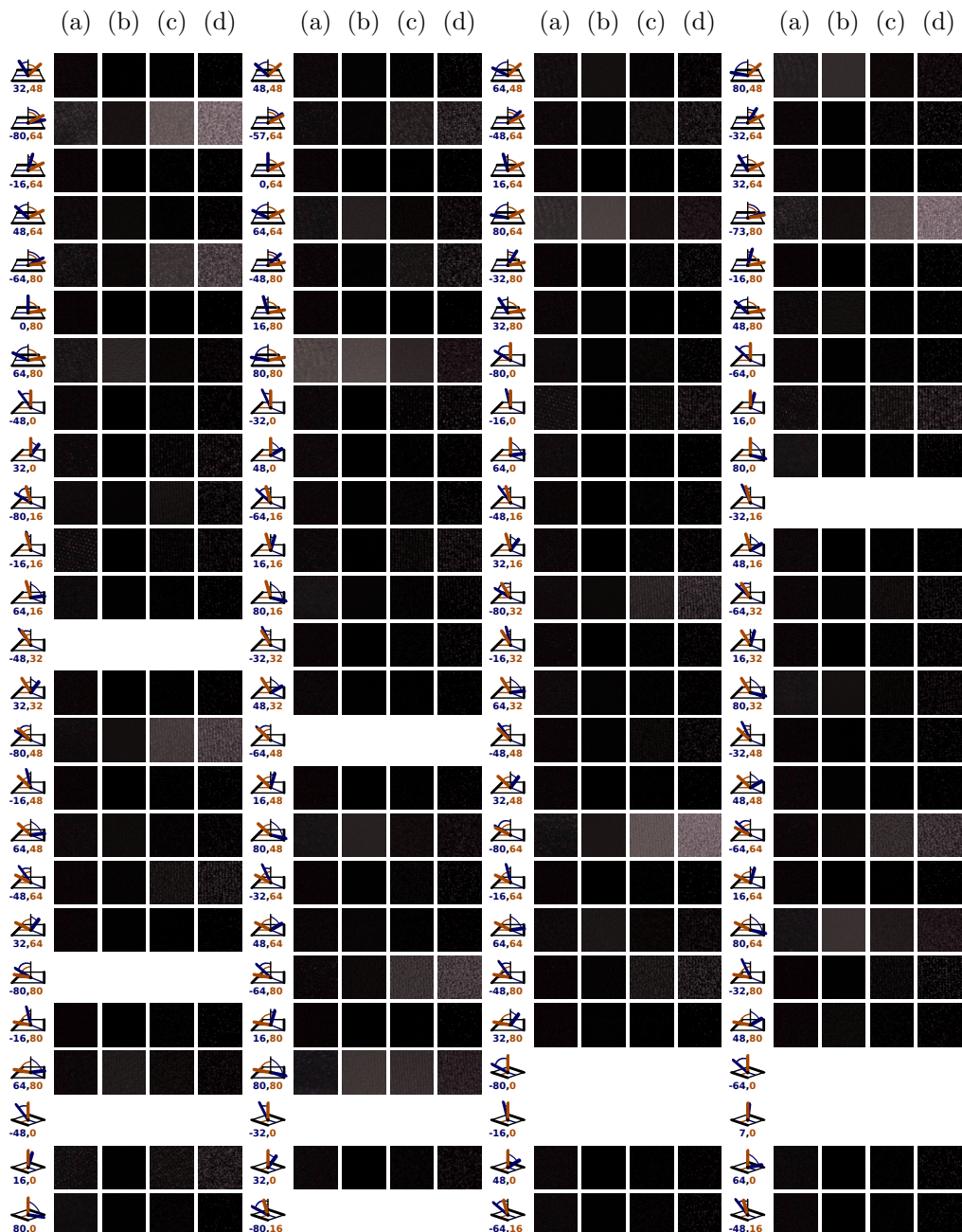


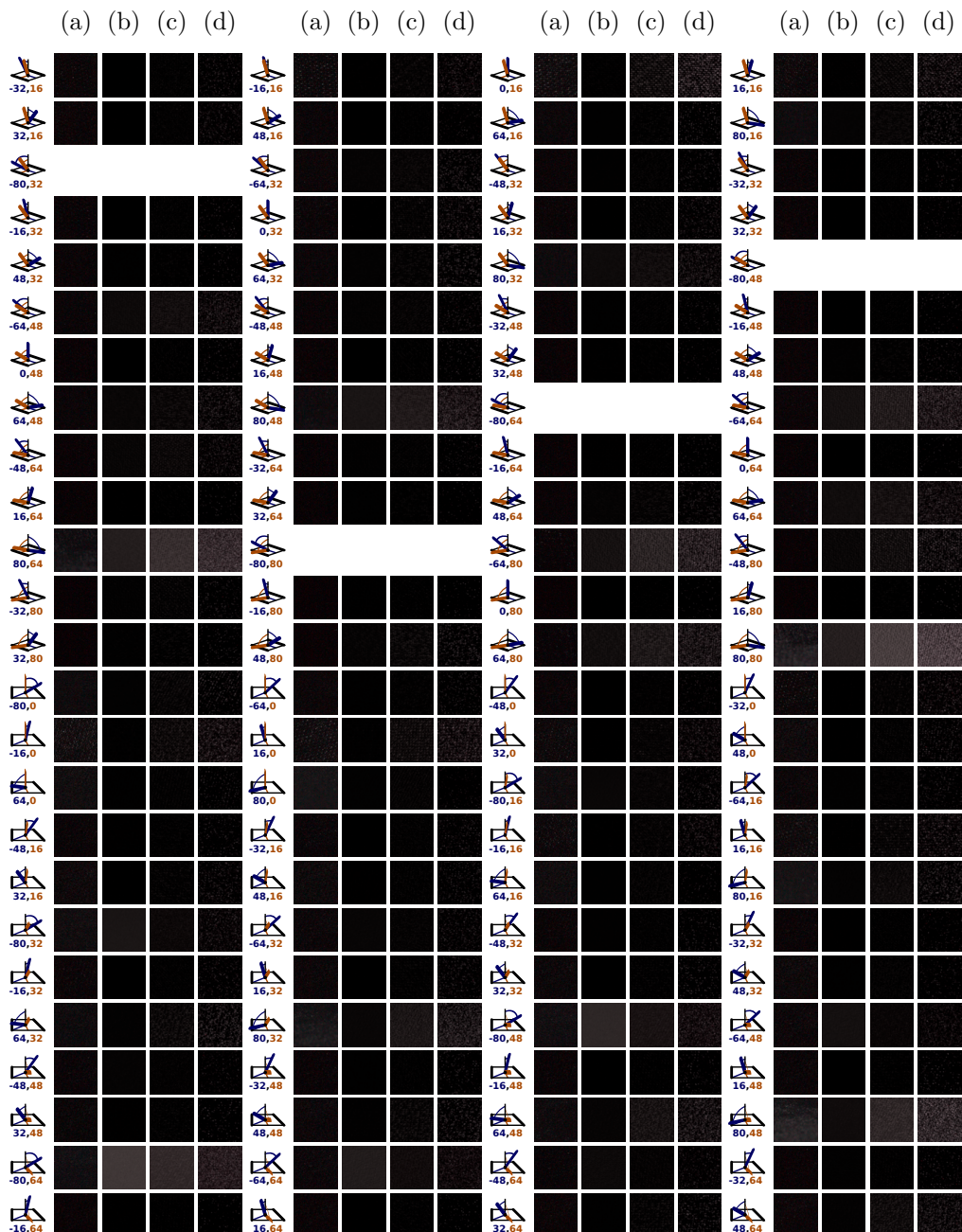


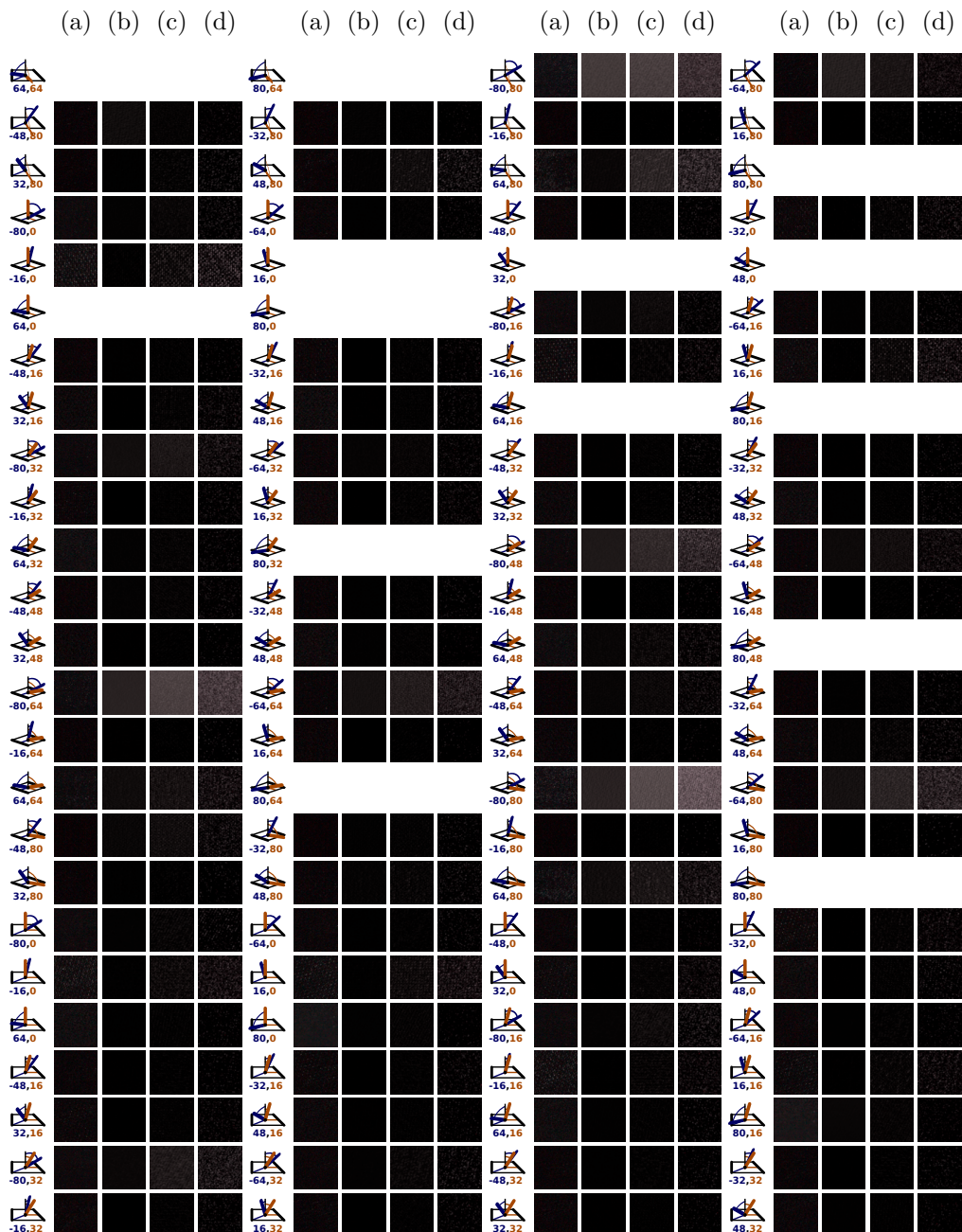


## 5.4 Velvet



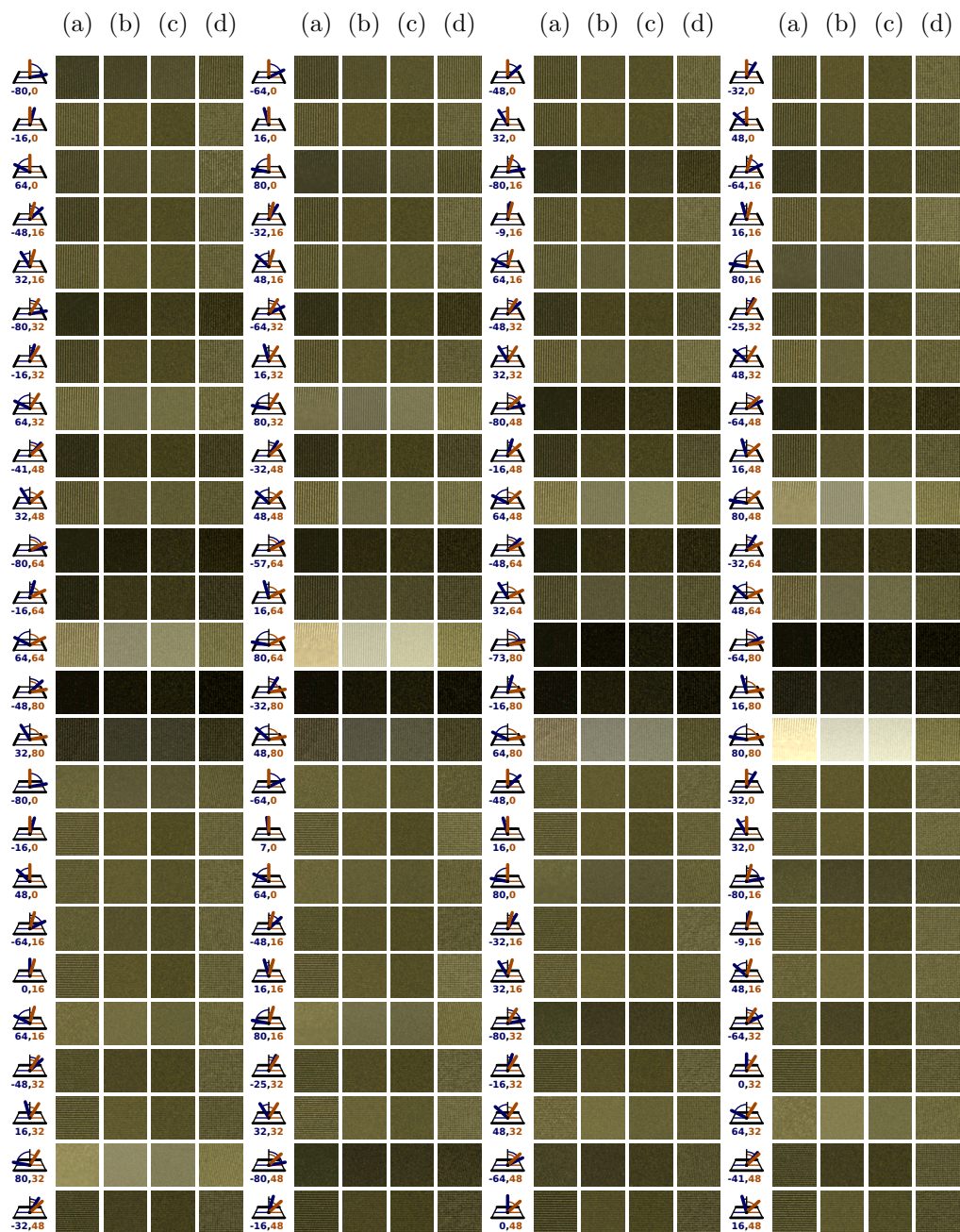


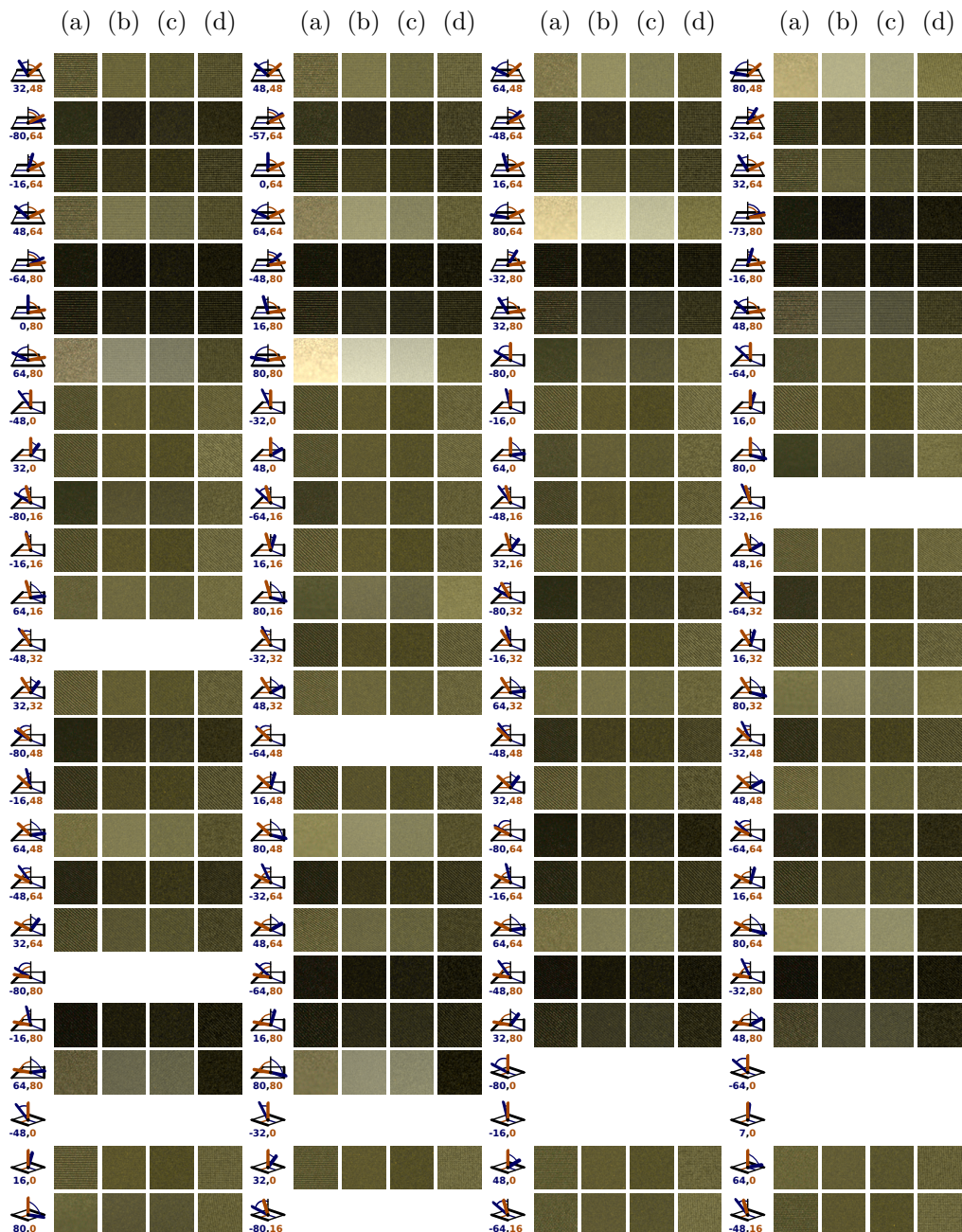




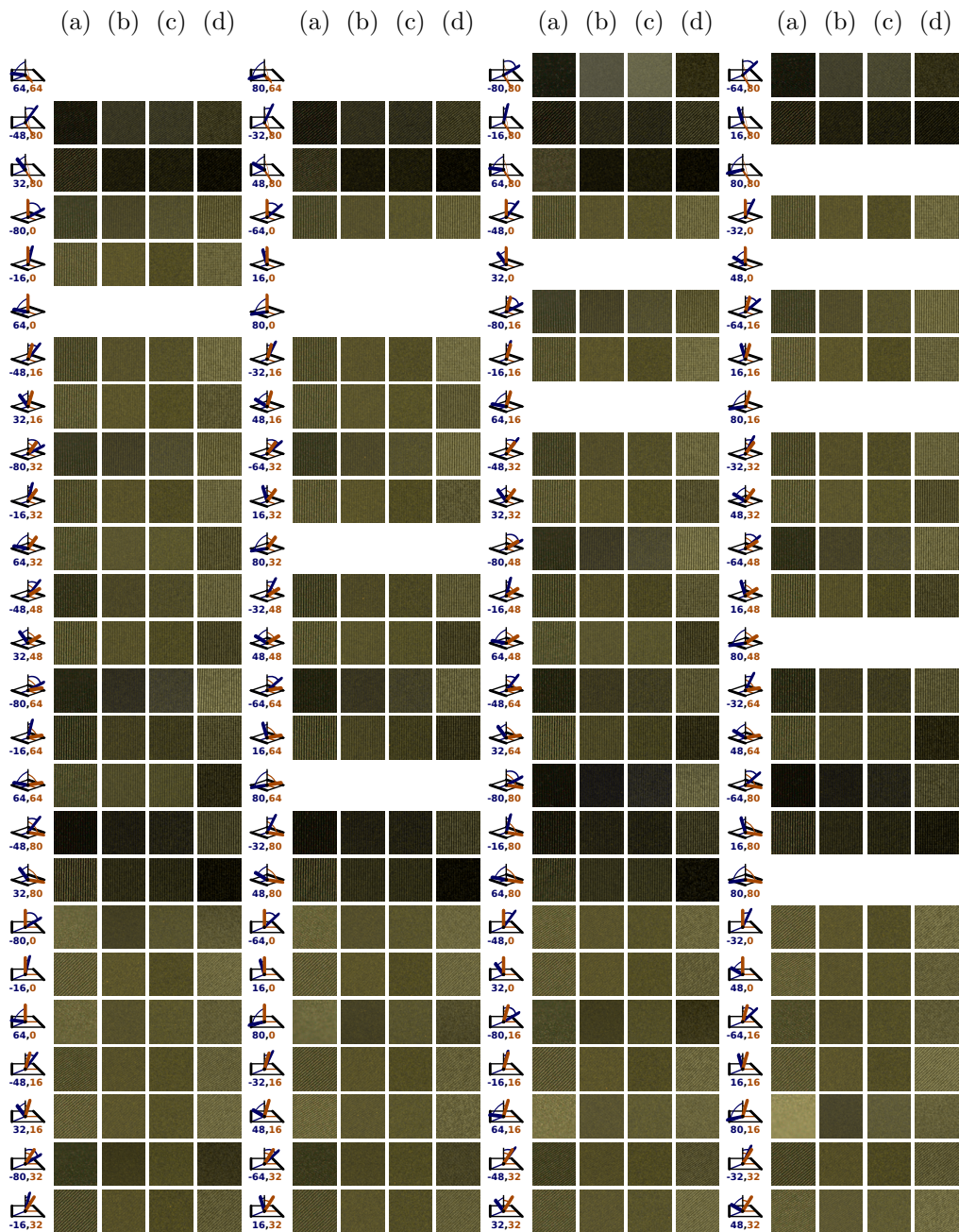


## 5.5 Twill







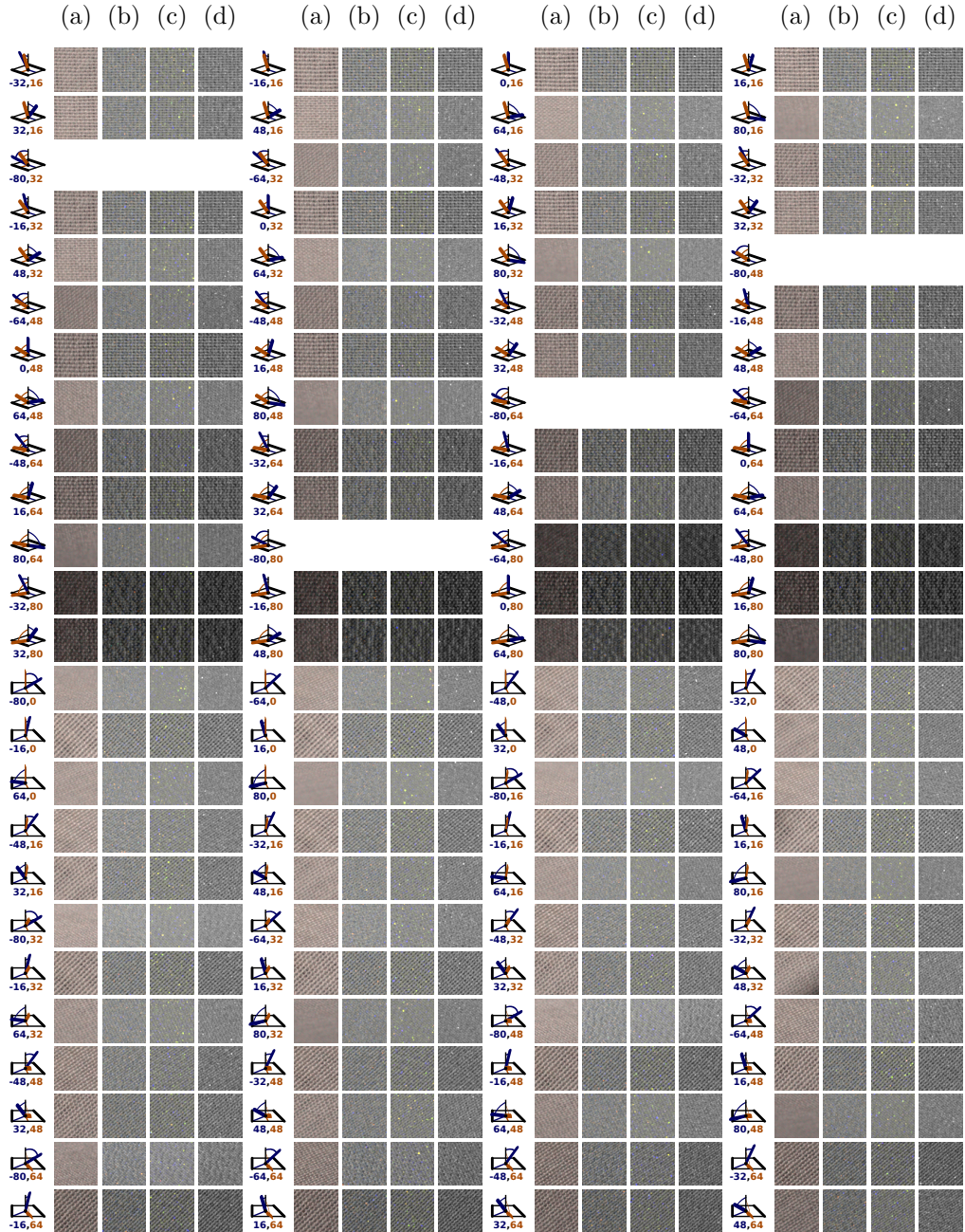




## 5.6 Cotton











## References

- [1] Pramook Khungurn and Steve Marschner. Azimuthal scattering from human hair fibers. Unpublished manuscript submitted to *ACM Transcations on Graphics*.